Rangsit Journal of Arts and Sciences, July-December 2012 RJAS Vol. 2 No. 2, pp. 161-174

Growing carbon nanotubes vertically and horizontally to the substrate: a review

Marguerite Ellis[1], Binh Duong[2], and Supapan Seraphin[1*]

[1]Department of Materials Science and Engineering, University of Arizona, Tucson, Arizona 85721, U.S.A.
E-mail: mellis@email.arizona.edu, seraphin@email.arizona.edu
[2]NanoScience Technology Center, University of Central Florida, Florida 32826, U.S.A.
E-mail: Binh.Duong@ucf.edu

*Corresponding author

Submitted 19 June 2012; accepted in final form 24 September 2012

Abstract

This review article provides information on processing conditions of chemical vapor depositions that are significant to the growth of carbon nanotubes (CNTs) either vertically or horizontally along the substrate. Carbon nanotubes are generated in forms of single-walled, double-walled, multi-walled cylindrical tubes, and stacked-cone fibers. Novel composites of vertically aligned CNTs and graphitic layer are also presented. Key processing parameters include type of catalyst systems, underlayer, gaseous hydrocarbon sources, and gas flow rate. Growth mechanisms of various CNT forms are discussed. The review includes Raman spectroscopy analysis to determine electrical and structural properties of CNTs.

Keywords: *carbon nanotubes, carbon nanofibers, double-walled carbon nanotubes, chemical vapor deposition of carbon nanotubes, Raman spectroscopy of carbon nanotubes*

1. Introduction

Allotropes of carbon, such as amorphous carbon, diamond and graphite, have quite different properties due to their dissimilar structures. Other allotropes of carbon exist and include fullerenes, carbon nanotubes (CNTs), carbon nanofibers (CNFs), and graphene and have attracted much attention over the past few decades due to the unique properties of each, making them suitable for a variety of potential applications. CNTs and CNFs can be produced by various techniques, each having advantages and drawbacks. Chemical vapor deposition (CVD) is perhaps the most popular method for growing CNTs/CNFs at specific locations and orientation (vertically v.s. horizontally) on a substrate, which is important for many applications. Requirements such as vertical alignment of the fiber axis with respect to the substrate and low temperature growth are necessary for applications in field emission devices and electronics. Although much progress has been made towards the ability to grow vertically aligned CNTs/CNFs on substrates, the need remains to obtain a better understanding of the complex interplay of various CVD processing parameters in order to have more control and reproducibility over the properties of CNTs/CNFs. Additionally, the recent report of self-assembled novel composites composed of vertically aligned CNT (VA-CNT) with multi-layered graphene produced by CVD (Kondo, Sato & Awano, 2008; Jousseaume, Cuzzocrea, Bernier, & Renard, 2011) has amplified the need for a better understanding of how the CVD processing parameters and catalyst system affect the structure of the graphene layers (or graphitic layer) (GL), the overall composite morphology and the structure of fibers (CNTs and/or CNFs). This article is to review the effects of CVD processing conditions such as types of substrate, catalyst systems, composition of the hydrocarbon source materials, and gas flow rates on the morphology and structure of vertically- and horizontally-grown CNTs and CNFs.

2. Historical background

The first fullerene, C_{60}, was observed by Kroto, Heath, O'Brien, Curl, and Smalley in 1985 and was named buckminsterfullerene, although it is more commonly called the buckyball. The discovery of CNTs is widely attributed to Sumio Iijima (1991). However, the early observation of carbon filaments occurring via catalytic decomposition was noted over a century ago; the method used to produce carbon filaments is described in an 1889 patent (Hughes & Chambers, 1889). These early carbon filaments

DOI : 10.14456/rjas.2012.26

generally include both CNTs and CNFs, but structural determination could not be performed until technological advances were made, such as the development of high-resolution transmission electron microscopy (TEM) (Nessim, 2010; Melechko, Merkulov, McKnight et al., 2005). More recently, graphene has come to the forefront with its "discovery" in 2004 by Konstantin Novoselov and Andrew Geim winning them the Nobel Prize in 2010 (Novoselov, Geim, Morozov et al., 2004).

3. The structure and the potential applications of graphene, CNTs, and CNFs

The structure of graphene can be described as a monolayer of sp^2 hybridized carbon atoms arranged hexagonally. Since 2004, graphene research has made rapid progress and has sparked interest in graphene/CNT composites. Graphene holds great promise for potential applications due to its strength, stability under ambient conditions, high quality and electronic properties (Novoselov et al., 2004).

CNTs and CNFs have been widely studied over the last two decades due to their unique electronic, optical and physical properties. There are two main categories of CNTs, single-walled CNTs (SWCNTs) and multi-walled CNTs (MWCNTs). The structure of a SWCNT can be thought as a graphene sheet rolled up to form a tube like structure that may be capped at one or both ends by a fullerene hemisphere. A SWCNT has different conformations-zigzag, armchair and chiral (Dresselhaus, Dresselhaus, & Eklund, 1996). SWCNTs can be metallic or semiconducting depending upon the conformation. SWCNT outer diameters can be less than 1 nm with aspect ratios that can exceed 1,000,000 (Nessim, 2010). MWCNTs can be thought of as rolled up sheets of graphene that are concentrically aligned, or as a set of SWCNTs nested one inside the other. The distance between walls in MWCNTs is about 0.34 nm, which is similar to the 0.335 nm spacing between the stacked graphene planes that compose graphite. MWCNTs can have two or more walls and have outer diameters from 1 – 100 nm and are typically metallic (Nessim, 2010).

The structure of a CNF differs from that of a CNT; however, this distinction is often overlooked in the literature. CNFs can be described as having either a cylindrical or conical structure composed of graphene sheets with lengths ranging from less than a micron to several millimeters and diameters on the order of a few up to hundreds of nanometers. In fact, Melechko et al. (2005) describes the CNT structure as a special case that falls under the category of CNFs. According to Melechko et al., the designation of a CNF as a CNT is based on the angle (α) between the graphene sheet of the sidewall and the tube axis [Figure 1(a)]. If the angle is zero, meaning that the tube wall(s) are parallel to the tube axis for the full length of the tube, then the tube is designated as a CNT. In comparison to the special case CNT structure, all other CNFs have side wall angles that are greater than $\alpha = 0$ [Figure 1(b)] that result in either a "stacked cone" structure or a "stacked cup" structure that resembles bamboo.

Although many researchers do not make a distinction between CNTs and other types of CNFs, such as the stacked cup or cone, it is quite clear that there is a distinct difference in their structures and hence their properties. However, it has been demonstrated that the properties of CNTs and/or CNFs make them desirable for numerous applications such as gas sensing (Valentini, Cantalini, Armentano et al., 2004), electroanalysis and biosensing (Huang, Liu & You, 2010; Wu, Zhang & Ju, 2007), hydrogen storage (Biris et al., 2008; Jang et al., 2005), field emission devices (Wang et al., 1998; Sveningsson et al., 2004; Chen et al., 1998; Sung et al., 2008; Poa et al., 2005; Park et al., 2005; Ma et al., 1999), and as additives in polymer nanocomposites (Vera-Agullo et al. 2009; Zhang et al., 2006; Linares et al., 2008).

In the CVD process, numerous CNTs and CNFs grow along the direction of the gas flow to the substrate. This results in a thin layer of vertical or horizontal tubes with respect to the substrate. Figure 2 shows an example of each type of vertical and horizontal CNTs to the substrate.

Recently, novel self-assembled composite films composed of VA-MWCNTs (Kondo, Sato & Awano, 2008; Jousseaume et al., 2011) combined with multiple layers of graphene, arranged perpendicular the CNTs'/CNFs' axes have been reported. The unique structures of these self-assembled composites are promising for various applications that would benefit from this type of architecture.

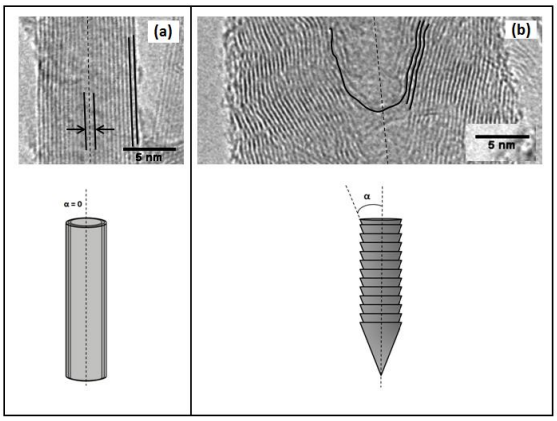

Figure 1 (a) High resolution TEM image of a MWCNT with an inner diameter of ~1 nm. The cartoon shows that the MWCNT structure is defined by the angle (α) between the graphene walls and the tube axis is equal to zero. (b) TEM image of a MWCNF with a stacked cone structure. Note the non-zero angle between the graphene walls and the fiber axis for the stacked cone type of MWCNF structure (Ellis, 2011). Cartoon diagrams based on (Melechko et al., 2005).

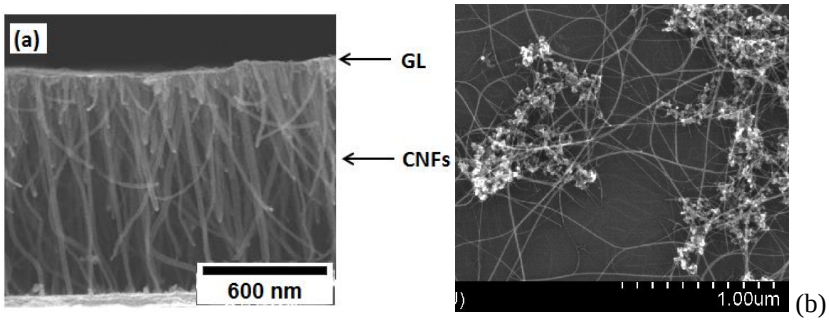

Figur 2 Scanning electron images of (a) vertically-grown CNTs (Ellis, 2011); (b) horizontally-grown CNTs. The round features are catalysts and other forms of carbon (Duong et al., 2011).

4. Raman spectroscopy of CNTs/CNFs

The essential purpose for establishing a controllable CNT growth is to ultimately achieve superior properties that have been theoretically determined. The extraordinary electrical properties of CNTs have drawn significant attention in the research community. Chirality and diameter are the two key factors in determining whether a nanotube is semiconducting or metallic (Dresselhaus, Dresselhaus & Eklund, 1996). Extensive effort has been taken to measure qualitatively the electrical properties of individual SWCNTs using Raman spectroscopy. Without sample preparation, fast and non-destructive analysis, Raman spectroscopy, can provide essential information on the type of nanotube SWCNTs vs. MWCNTs), diameter, electrical properties (metallic vs. semiconducting features), chiralities, and defects. As shown in Figure 3, the position, shape, width, and relative intensity of Raman spectra are modified according to the types of CNTs (Dresselhaus et al., 2010; Costa et al., 2008; Dresselhaus, Dresselhaus, Saito, & Jorio, 2005).

Some of the characteristic features of a Raman spectrum for CNTs are the radial breathing mode region (RBM, frequency <300 cm^{-1}), the defect/disorder band (D-band, ~1200-1400 cm^{-1}) and the graphite band (G-band, ~1500-1600 cm^{-1}). The tube diameters, d_t, could be calculated from the RBM frequency, ω_{RBM}, using the formula $d_t = A/\omega_{RBM}$, where A is determined experimentally. Multiple values of A have been reported: 223 nm cm^{-1} (Rao et al., 1997), 218 nm cm^{-1} (Jishi et al., 1993), 234 nm cm^{-1} (Kurti, Kresse & Kuzmany, 1998), 236 nm cm^{-1} (Sanchez-Portal et al., 1999), 227 nm cm^{-1} (Mahan, 2002) and 248 nm cm^{-1} (Jorio

et al., 2001). The average diameter of nanotubes can also be characterized by analyzing the shape of the G-band, however, it is not as accurate as the information extracted from the RBM region. Several studies, as shown in Figure 4**,** have established the relationship between the RBM and the diameter of a nanotube. It should be noted that the intensity of RBM is too weak to be observed for nanotubes with diameters greater than 3 nm (Dresselhaus et al., 2010).

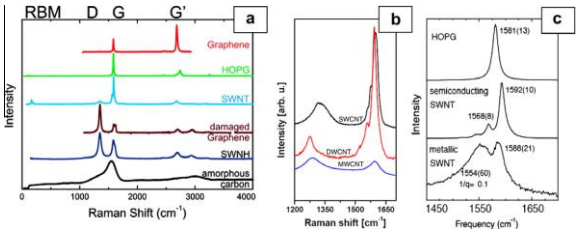

Figure 3 (a) Typical Raman spectrum of CNTs; (b) D and G bands of SWCNTs, DWCNTs and MWCNTs; and (c) the G-band for highly-oriented pyrolytic graphite (HOPG), semiconducting and metallic SWCNTs. (Dresselhaus et al., 2010; Costa et al., 2008; Dresselhaus, Dresselhaus, Saito, & Jorio, 2005)

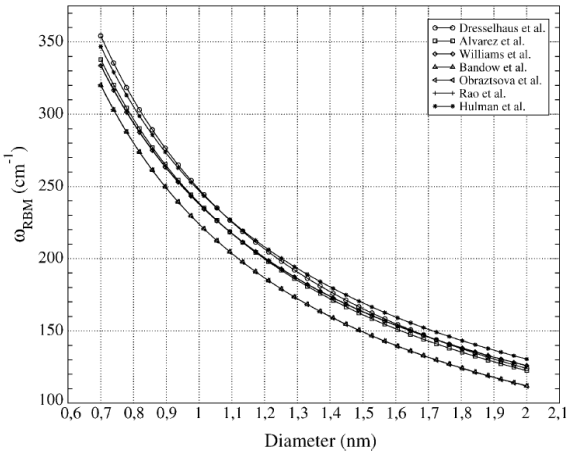

Figure 4 Phenomenological relations between RBM Raman mode and the nanotube diameter as determined by several authors (Belin and Epron, 2005).

Defect information can easily be extracted by analyzing the position and linewidth of the D-band. For instance, amorphous carbon has a very broad linewidth of more than 100 cm^{-1}, whereas crystalline graphite has a typical position of 1305-1330 cm^{-1} and a width of ~30-60 cm^{-1} (Wang, Alsmeyer & McCreery, 1990). Quality (degree of crystallinity) of an as-grown batch of CNTs can be determined by taking the intensity ratio of the D-band to G-band. The most important feature in a Raman spectrum is the G-band. It corresponds to a tangential vibration mode along the graphitic plane of a nanotube. The multi-peak and fine features in the G-band contain qualitative electrical information about the CNTs as shown in Fig. 3(c). Information about nanotube chiralities can be obtained by analyzing the lineshape and frequency of G-band and/or RBM (Belin and Epron, 2005). For SWCNTs, the differences in lineshapes of the G-band is particularly sensitive for tubes with diameters d_t<1.7 nm. Although not as much information can be gleamed from the Raman spectra for MWCNTs/MWCNFs, the quality of the carbon structure can be assessed. For MWCNTs and MWCNFs, the dominant Raman modes are the G-band (around 1500-1600 cm^{-1}) and the D-band (around 1250-1450 cm^{-1}). The G-band (graphite) correlates to the order and symmetry of the carbon structure and the D-band (disorder) relates to the disorder and indicates the presence of defects (Liu, Pan & Wang, 2004). The ratio of the intensity of the D-band (I_D) to the intensity of the G-band (I_G) provides information about the degree of order, or quality of CNTs/CNFs. The I_D/I_G is sometimes referred to as the R-factor. A large value for the R-factor indicates a high degree of disorder, while a small value R-factor value implies a more ordered and highly purified structure (Liu, Pan & Wang, 2004; Malesevic et al., 2007).

G^+ peak corresponds to the higher frequency component of the G-band. It is less important since it does not directly depend on the diameter of nanotubes. G' corresponds to the second overtone of the defect-induced D mode. The G' position depends on diameter of SWCNTs and can be used roughly to estimate the value. G' mode of double-walled CNTs is a doublet. However, it is often unresolved due to line broadening (Dresselhaus, Dresselhaus, Saito, & Jorio, 2005).

While Raman proves to be a powerful technique to characterize CNTs, it remains a challenge to simultaneously observe as-grown nanotubes and pinpoint their electrical properties.

5. Key processing methods to grow CNTs/CNFs

CNTs and CNFs are produced by various methods such as arc discharge (Iijima, 1991; Jiao &

Seraphin, 1998), laser ablation (Guo et al., 1995), high-pressure carbon monoxide conversion process (Sivakumar et al., 2010) and various chemical vapor deposition (CVD) techniques (Nessim, 2010; Melechko et al., 2005). Here, only the CVD method is reviewed.

CVD is a very popular processing method because it is a relatively simple technique that is economical and well suited for large-scale production of CNTs/CNFs (Sivakumar et al., 2010). The CVD process allows the growth of CNTs/CNFs directly on a substrate at relatively low temperatures making it suitable for use in electronic or complementary metal-oxide-semiconductor (CMOS) applications (Nessim, 2010). The ability to grow CNTs/CNFs at low temperatures is also important when a low thermal budget material, such as soda lime glass, is used as a supporting substrate. The softening temperature of soda lime glass is near 550 °C (Honda et al., 2006; Takeda et al., 2005) so it is necessary to be able to produce CNTs/CNFs at lower temperatures than this.

Potential applications such as bio and chemical sensing (Huang, Liu & You, 2010) and field emission devices require the growth of vertically aligned CNTs/CNFs (VA-CNTs/VA-CNFs) that are arranged perpendicular to the support layer (or substrate surface). Currently, the CVD method is the only synthesis method that allows control over the placement and alignment of CNTs/CNFs on a substrate (Nessim, 2010; Melechko, 2005).

There are various types of CVD methods, but two of the most popular types for growing CNTs are thermal CVD (TCVD) and plasma-enhanced CVD (PECVD). Although PECVD is successfully used at relatively low temperatures to grow VA-CNTs/VA-CNFs, in terms of scaling up, this method is not easily able to produce uniform CNTs over large substrate areas due to plasma instability. In contrast, state-of-the-art TCVD technology allows for the fabrication of CNTs over large areas, although commonly at higher temperatures. TCVD is often performed at atmospheric pressure but can also be carried out at low pressure (LPCVD). LPCVD is useful for controlling the packing density of vertically-aligned CNTs (important for certain types of applications), which is achieved by minimizing the carbon supply and controlling the growth rates.

5.1 Types of CVD processes

In general, growth of CNTs/CNFs by the CVD process involves the catalytic decomposition of carbon source gas(es) (methane, acetylene, ethylene, carbon monoxide, etc.) on metal(s) (typically transition metals such as Fe, Ni and Co). Other gases, such as nitrogen, argon, ammonia, hydrogen, are often used in the process to act as the carrier, diluting, etchant, doping or reducing gas(es). Processing temperatures are usually in the range of 400 °C to 1000 °C.

There are two types of methods used to introduce the catalyst: 1) a floating catalyst method where the catalyst is typically supplied from a gas source during the CVD process (no substrate used) and 2) the supported catalyst method where the catalyst is deposited on a substrate prior to the initiation of CNT/CNF growth. In this review, only the supported catalyst method will be discussed.

The typical apparatus used for TCVD consists of a quartz tube placed within a tube furnace through which carbon source gas(es) and/or other gases (Ar, N_2, H_2, etc.) flow (Figure 5). Since TCVD is typically performed at atmospheric pressure, the TCVD parameters that must be considered are the temperature, growth time, gas types (carbon source and co-gas(es)), gas flow rates and the ratio of source gas to co-gas. Other parameters involved, such as the substrate, catalyst, catalyst underlayer system and catalyst pre-treatments, must also be considered and will be discussed further in the next section.

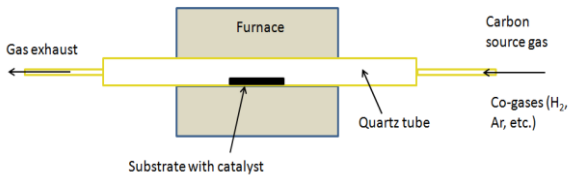

Figure 5 Cartoon schematic showing a typical tube-furnace-type TCVD system for growing horizontally CNTs/CNFs. Note that the direction of gas-flow is along the same direction of the substrate. Fig. based on Melechko et al., 2005.

PECVD is similar to TCVD, but the heat for the reaction is not supplied by thermal means. Instead, plasma is generated that activates the gas molecules by electron impact and thus reduces the activation energy for carbon deposition, which can allow growth at lower temperatures. A typical PECVD apparatus is shown in Figure 6. It is important to mention that there are several sub-categories of PECVD based on the type of plasma

generation used. These include hot-filament dc, microwave, magnetron type radio frequency, inductively coupled plasma, etc. Complexity of CVD parameters increase with the PECVD process, due to the plasma environment. For instance, the current and voltage setting affects the plasma power. The total pressure and the ratio of the source gas to the "etchant" gas must also be carefully controlled. By varying the temperature and the ratio of the carbon source gas (acetylene, C_2H_2) to the etchant gas (ammonia, NH_3), and holding all other parameters constant, Melechko et al. showed that growth of VACNFs is significantly affected by the C_2H_2:NH_3 ratio with respect to temperature. The results ranged from graphitic carbon (increased ratio of carbon), to high quality VACNF growth (optimal C_2H_2:NH_3 ratios), to CNF remnants (due to etching effects from increased ratio of NH_3). The range of optimal ratios for C_2H_2:NH_3 was dependent upon temperature. To simplify the process in many applications, a plasma reactor was usually used without plasma generation.

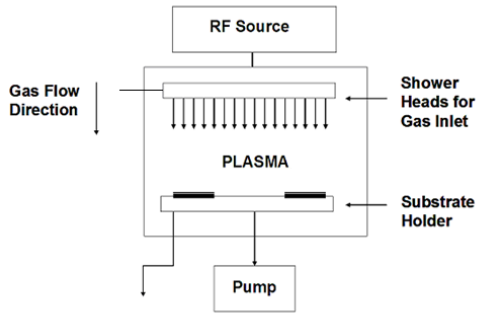

Figure 6 Diagram of a typical plasma-enhanced CVD (PECVD) apparatus for growing vertically-aligned CNTs/CNFs. Note that gas flows perpendicular to the substrate in contrast to Figure 5. (Jutarosaga et al., 2006).

5.2 CVD processing parameters

5.2.1 Substrate, catalyst and catalyst underlayer

Some of the most common substrates used for CVD include quartz, silicon (Si), Si with a SiO_2 layer, and alumina. The active catalyst is usually a transition metal such as Ni, Co or Fe that is deposited onto the substrate by physical deposition or other methods. There are many other catalysts that can also be used including binary or multi-metal alloys. When a catalyst is deposited directly onto a Si substrate, a silicide can form that may inhibit CNT/CNF growth (Melechko et al., 2005). Therefore, an oxide layer is often produced on the Si substrate by thermal oxidation to act as a barrier to prevent silicide formation.

The synthesis of both SWCNTs and MWCNTs using transition metals such as Fe, Ni, Co, and Pd has become a routine process, which sometimes leads to a misconception that these metal catalysts are required for the formation of CNTs. During the past ten years, increasing attention has been made to search for new catalysts for nanotube growth. For instance, it has been shown that different metals such as Au (Bhaviripudi et al., 2007; Takagi et al., 2008), Ag, Mn, Mo, Sn, Mg, Al and Pt (Yuan et al., 2008), Cu (Zhou et al., 2006; Ding et al., 2008; Ding et al., 2009), and Rh can be used as catalysts. Additionally, various semiconductors and oxide nanoparticles such as Si, Ge, SiO_2, TiO_2, Al_2O_3, La_2O_3 and Er_2O_3 (Liu et al., 2009; Huang et al., 2009) have also proved active for SWCNT growth. Recently, Takagi et al. (2008) reported successful growth of SWCNTs using carbides such as SiC and Fe_3C. The new findings regarding these various catalysts indicated that the size of the catalyst is more critical in the formation of CNTs than the catalyst type. In other word, CNTs can be grown on almost any suitably sized materials (Huang et al., 2009) and the goal of many current research efforts is to find a suitable size for each catalyst to obtain high efficiency growth.

It is often assumed in the CNT growth model by CVD process that one catalyst-seed nucleates one nanotube; hence, the diameters of the nanotubes are determined by the sizes of the catalyst particles (An et al., 2002). It has been suggested that uniform nanotubes can be achieved if monodisperse catalyst nanoparticles are used. Although researchers have been able to produce a narrow diameter distribution of CNTs (Choi et al., 2002; Jeong et al., 2005), it is often found that the majority of particles were not nucleating nanotubes. It has been proposed that under a given growth condition where carbon feeding and temperature are fixed, there is an optimal diameter of catalyst particles to nucleate CNTs (Lu & Liu, 2006). According to this hypothesis, particles whose diameter is larger than that of optimal one are inactive due to "underfeeding" (Figure 7), whereas smaller particles are poisoned due to "overfeeding". In "overfeeding" excessive carbon feeding creates a graphite shell, which inhibits the CNT nucleation. The "underfeeding" situation requires further investigation because the experimental study showed that large nanoparticles did not nucleate, even after

prolonging growth time to allow the particles to collect more carbon. Interestingly, it has been reported that when varying the growth temperature (Bachilo et al., 2003; Miyauchi et al., 2004), polydisperse catalyst particles can produce relatively uniform nanotubes and insignificant variations in the diameter of the nanotubes. These results indicate a more complex view of controllable and efficient CNT growth than the simple idea that the diameter of nanotubes is a function of catalyst size. Several studies found that for better growth efficiency, it is more critical to optimize other growth parameters such as growth temperatures and hydrocarbon feeding rates (Lu & Liu, 2006; Zhou, Ding & Liu, 2009, Li et al., 2010). It was shown that systematically controlling the carbon feeding rates can achieve uniform small diameter nanotubes even when highly polydisperse nanoparticles were used. In the following section, the effects of different hydrocarbon sources will be reviewed.

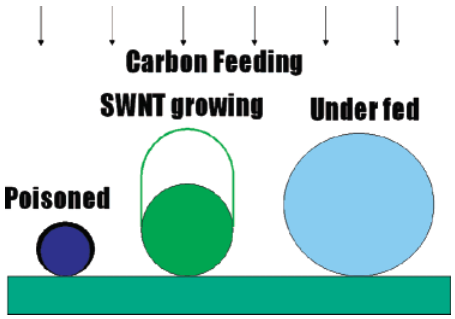

Figure 7 Activation of nanoparticles is determined by their diameters under a given carbon feeding rate. Larger particles are underfed and not nucleating growth, while smaller particles are cut-off from carbon supplies by one or more layers of graphene sheet (the black layer in this Figure). Only particles with a moderate and suitable size can nucleate growth (Lu & Liu, 2006).

In the case where the active catalyst and/or metal underlayers are deposited onto the substrate using physical deposition methods, the active catalyst becomes oxidized upon exposure to ambient conditions. It is often important for the thin film to undergo a pre-growth treatment in order to form discrete catalyst nanoparticles, which serve to nucleate the growth of CNTs/CNFs. The pre-treatment of the catalyst system can be performed in various ways such as H_2 plasma treatment (Yen et al., 2004), or annealing in the presence of reactive gases, such as NH_3 (Lee et al., 2001), or H_2 (Yen et al., 2004). Alternatively, annealing is done in the presence of an inert gas, such as Ar (Labunov et al., 2010). It is also possible for the catalyst thin film to become reduced during the growth process when reducing gases such as NH_3 or H_2 are used in conjunction with the carbon source gas(es). Another method that is used in order to preclude the necessity of catalyst pre-treatment is the use of metal underlayers (Delzeit et al., 2002).

Metal underlayers are deposited between the substrate and the catalyst layer. The metal underlayer can serve various functions: 1) it can act as a barrier layer between the substrate and the catalyst, thereby preventing silicide formation (Melechko et al., 2005); 2) it can be useful for electronic applications that require a conductive underlayer and for devices that are fabricated using current CMOS technology (Sun et al., 2010; Delzeit et al., 2002); 3) it may provide surface roughness and thereby increase active catalyst nucleation sites, thus eliminating the need for pre-treatment of the active catalyst (Delzeit et al., 2002) and 4) it may act as an adhesion layer that creates a stronger interaction between the catalyst and substrate creating a stronger interaction resulting in base type growth of CNTs/CNFs. On the other hand, it is more difficult to grow CNTs/CNFs on metallic underlayers due to the possibility of alloy or intermetallic compound formation. The thickness of the catalyst layer and the interaction with the substrate or underlayer will influence the coarsening and dewetting and thus affect the structure of the CNT/CNF.

It was found that the morphology and structure of MWCNF/GL composites varies significantly with the catalyst underlayer system used (Ellis et al., 2012). The morphology and quality of the composites are found to be affected by the type of dilution gas used and/or by the dilution gas flow conditions. The effect of the dilution gas varies with the catalyst underlayer system. The effect of the underlayer system on the morphology and structure of the films is thought to be due to interactions between the catalyst and underlayer due to wetting behavior, catalyst diffusion, possible inter-metallic compound formation and thermal stresses.

Raman analysis complemented TEM analysis by signaling the presence of MWCNTs with very small inner diameter (< 1 nm) which led to the detection of a combined MWCNT, MWCNF and GL composite produced using one of the catalyst underlayer systems. The presence of Au in the underlayer system contributed to increase MWCNF density, vertical alignment and length.

In many applications of CNTs, one would prefer to get rid of metallic catalyst particles from the vertically-aligned CNTs. A report by Hata et al. (2004) demonstrated a water-assisted CVD synthesis to grow dense and vertical nanotube forests with heights up to several millimeters. The CNTs film was cut from the catalysts with a knife (Gong, K,; Chakrabarti, S., Dai, L. 2008). Du et al. (2011) showed a method to make epoxy composite membranes of the vertically-aligned CNTs. They also developed a magnetic-nanoparticle switching system to turn on and off the liquid flowing through the nanotube memberanes by using an alternating voltage. Recently, Duong et al. (2012) reported a method to grow MWCNTs using polyacrylonitrile as a solid carbon source and nanosized SiO_2 particles as catalyst. The nanotubes can be grown either on a silicon substrate or as a freestanding film at temperature as low as 800ºC.

5.2.2 Selection of gaseous hydrocarbon sources

Extensive studies have been carried out to investigate the role and impact of different carbon precursors on CNTs. Some of the most commonly used hydrocarbons are methane (Kong et al., 1998; Franklin & Dai, 2000), ethylene (Fan et al., 1999 and Satiskumar, Govindaraj & Rao, 1999), acetylene (Baker & Waite, 1975; Li et al., 1996), benzene (Sen, Govindaraj & Rao, 1997), xylene (Wei et al, 2002) and carbon monoxide (Nikolaev et al., 1999). Kong et al. (1998) reported individual SWCNTs at 900^{o}C from pyrolysis of methane. They found that carbon atoms decomposed from methane do not interact with other decomposed species such as H_2, C_2 or C_3. Furthermore, methane undergoes very little self-pyrolysis at high temperature, which prevents the formation of amorphous carbon on the nanotubes. Cheng et al. (1998) and Endo et al. (1993) synthesized SWCNTs from benzene at 1100-1200^{o}C whereas Jose-Yacaman et al. (1993) produced MWCNTs at 700^{o}C from acetylene. It should be noted that benzene pyrolysis occurred at a much higher temperature and generated a large amount of amorphous carbon during its pyrolysis. A systematic study by Li et al. (2004), on the effects of different hydrocarbon sources (methane, hexane, cyclohexane, benzene, naphthalene, and anthracene) using a CVD process between 500 and 850^{o}C, found that methane was more chemically stable than the other carbon sources and was most likely to yield high-purity SWCNTs.

It is important to emphasize that the molecular structure of the hydrocarbon has a strong impact on the morphology of the CNTs. CNTs grown by pyrolysis of a linear hydrocarbon, such as methane or ethylene are often straight because these carbon precursors thermally decompose into atomic carbon or linear dimers/trimers of carbon (Kumar & Ando, 2010). Benzene, xylene and other cyclic hydrocarbons produce relatively curved/hunched CNTs with tube walls often bridged inside. Therefore, the proper selection of a carbon precursor can significantly improve both the yield and quality of CNTs.

5.2.3 Effects of hydrogen flow rate on carbon nanotube growth

It is found that the variation of H_2 gas concentration and a set growth time of 15 minutes have a significant effect on the distribution, morphology, internal structure, and electronic properties of the nanotubes (Reynolds, Duong & Seraphin, 2010). The results revealed substantial quantity trends as hydrogen flow rates increased from 100 to 700 standard cubic centimeters per minute (sccm). At a constant CH_4 flow rate of 700 sccm, and varied H_2 of 100 and 200 sccm, few CNTs were produced. The highest density of CNTs was grown between H_2 flow rates of 300 and 400 sccm, as shown in Figure 8, thus suggesting optimum growth conditions within that range. Increasing H_2 to 700 sccm, decreased the amount of CNTs. The results can be used to guide a production process to obtain high quantity and quality CNTs with desired properties.

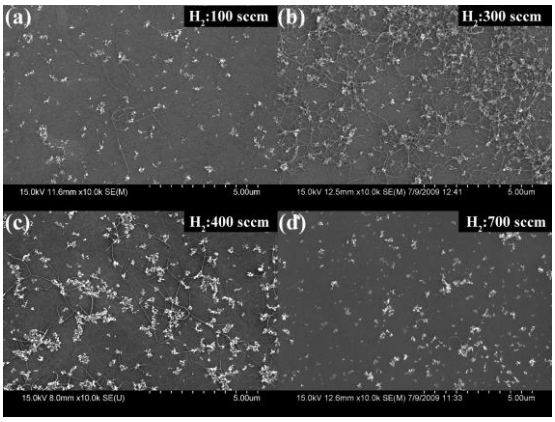

Figure 8 SEM images of CNTs grown at a hydrogen flow rate of (a) 100 sccm; (b) 300 sccm; (c) 400 sccm; (d) 700 sccm. (b) and (c) contain the highest density CNTs.

Duong et al. (2011) reported the internal structures and properties of CNTs that change with respect to the methane flow rates. They suggested that the nanotube density increases with increased methane flow rate. MWCNTs with metallic properties were obtained at methane flow rates as low as 300 cc/min. At higher methane flow rates, i.e. 600-700 cc/min, semiconducting SWCNTs and DWCNTs (as shown in Figure 9) were produced.

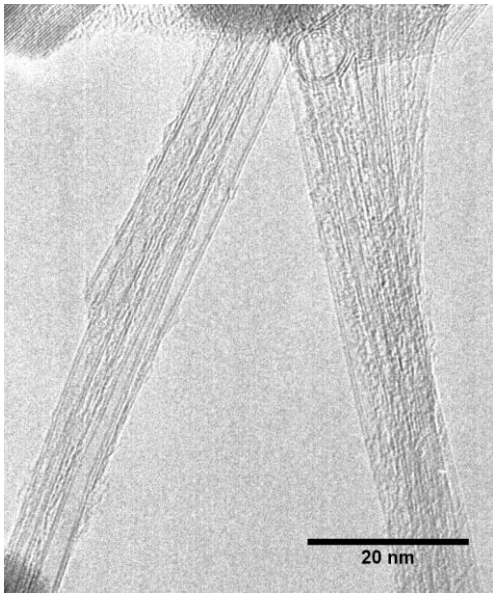

Figure 9 High-resolution TEM image of bundles of double-walled CNTs. (Duong et al. 2011).

6. Growth mechanisms of CNTs/CNFs for the CVD process

The growth mechanisms for CNTs/CNFs has been widely studied and debated. Overall, it is generally accepted that growth occurs by the following mechanism i) the hydrocarbon molecules adsorb and decompose on the catalyst surface, ii) diffusion of carbon species occurs through bulk and/or surface diffusion through the catalyst particle, iii) the precipitation of excess carbon nucleates the CNT/CNF structure (Nessim, 2010; Melechko et al., 2005). Two widely accepted growth models exist in the case of a supported catalyst, 1) tip growth and 2) base growth (Baker, 1989). In general, the type of growth that occurs is driven by the interaction between the catalyst and the substrate (or underlayer). This is thought to be due to the wetting of the catalyst particles and can be characterized by the contact angle between the catalyst nanoparticle and the catalyst support. If the interaction is weak (large contact angle), the CNT/CNF will grow by a tip growth method (Hofmann et al., 2005) in which the catalyst particle loses contact with the substrate and is pushed upward as the CNT/CNF forms beneath [Figures 10(a) and 11(a)]. On the other hand, if the interaction is strong (small contact angle) the growth proceeds by a base growth method. In the case of base growth, the catalyst particle remains in contact with the catalyst support while the CNT/CNF forms above the catalyst particle [Figures 10(b) and 11(b)].

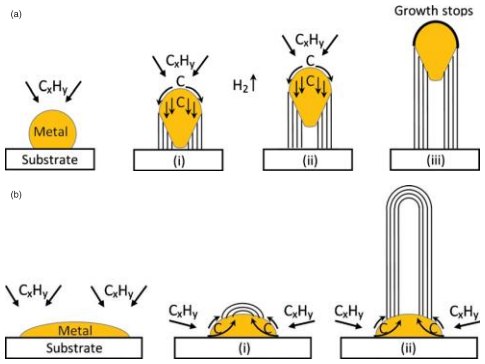

Figure 10 Widely-accepted growth mechanisms for CNTs: (a) tip-growth model, (b) base-growth model (Kumar and Ando, 2010).

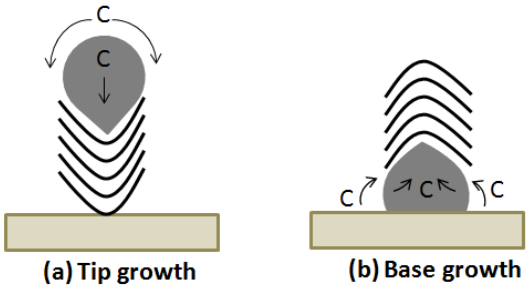

Figure 11 A simplified cartoon showing (a) tip growth mechanism and (b) base growth mechanism for CNFs.

7. Summary

The article reviews the growth of vertical and horizontal CNTs. Many forms of CNTs can be grown including single-walled, double-walled, multi-walled, and composites of vertically-aligned multi-walled fibers (VA-MWCNF)/graphitic layers (GL). Electron microscopy was used to identify their

morphologies and to identify different types of MWCNF composite structures produced using various CVD parameters and catalyst underlayer systems. Raman analysis was used to determine the CNT electrical properties and the quality of MWCNF composites. Various growth mechanisms for CNTs were reviewed.

8. Acknowledgements

The authors would like to acknowledge support from the National Science Foundation grants (Graduate Research Fellowship, DMR0243847, and EEC0812072) and a TRIF Imaging Fellowship from the Arizona Technology Research Infrastructure Fund.

9. References

An, L., Owens, J.M., McNeil, L.E., & Liu, J. (2002) Synthesis of nearly uniform single-walled carbon nanotubes using identical metal-containing molecular nanoclusters as catalysts, *J. Am. Chem. Soc. 124*, 13688-13689.

Bachilo, S. M., Balzano, L., Herrera, J. E., Pompeo, F., Resasco, D. E., & Weisman, R. B. (2003) Narrow (n,m)-distribution of single-walled carbon nanotubes grown using a solid supported catalyst, *J. Am. Chem. Soc.*, *125*, 11186-11187.

Baker, R. T. K., & Waite, R. J. (1975) Formation of carbonaceous deposits from the platinum-iron catalyzed decomposition of acetylene, *J. Catalysis, 37*, 101-105.

Baker, R.T.K. (1989) Catalytic growth of carbon filaments. *Carbon, 27*, 315-323.

Belin, T., & Epron, F. (2005) Characterization methods of carbon nanotubes: a review, *Mater. Sci. Eng. B, 119*, 105-118.

Biris, A.R., Lupu, D., Dervishi, E., Li, Z., Saini, V., Saini, D., et al. (2008) Hydrogen storage in carbon-based nanostructured materials. *Particulate Science and Technology: An International Journal*, *26*, 297-305.

Bhaviripudi, S., Mile, E., Steiner, S. A., Zare, A. T. Dresselhaus, M. S., Belcher, & A. M., Kong, J. (2007) CVD synthesis of singe-walled carbon nanotubes from gold nanoparticle catalysts, *J. Am. Chem. Soc.*, *129*, 1516-1517.

Chen, Y., Patel, S., Ye, Y., Shaw, D.T., & Guo, L. (1998) Field emission from aligned high-density graphitic nanofibers. *Appl. Phys. Lett.*, *73*, 2119-2121.

Cheng, H. M., Li, F., Su, G., Pan, H. Y., He, L. L., Sun, X., & Dresselhaus, M. S. (1998) Large-Scale and Low-Cost Synthesis of Single-Walled Carbon Nanotubes by the Catalytic Pyrolysis of Hydrocarbons. *Appl. Phys. Lett.*, *72*, 3282–3284.

Choi, H. C., Kim, W., Wang, D. W., & Dai, H. J. (2002) Delivery of catalytic metal species onto surfaces with dendrimer carriers for the synthesis of carbon nanotubes with narrow diameter distribution. *J. Phys. Chem. B, 106*, 12361-12365.

Costa, S., Borowiak-Palen, E., Kruszynska, M., Bachmetiuk, A., & Kalenczuk, R. J. (2008) Characterization of carbon nanotubes by Raman spectroscopy, *Mater. Sci. Poland*, *26*, 433-441.

Delzeit, L., Nguyen, C.V., Chen, B., Stevens, R., Cassell, A., Han, J., et al. (2002) Multiwalled Carbon Nanotubes by Chemical Vapor Deposition Using Multilayered Metal Catalysts. *J. Phys. Chem. B, 106*, 5629-5635.

Ding, L., Tselev, A., Wang, J. Y., Yuan, D. N., Chu, H. B., McNicholas, T. P., Li, Y., & Liu, J. (2009) Selective growth of well aligned semiconducting single-walled carbon nanotubes. *Nano Lett.*, *9*, 800-805.

Ding, L., Yuan, D. N., & Liu, J. (2008) Growth of high-density parallel arrays of long single-walled carbon nanotubes on quartz substrates. *J. Am. Chem. Soc.*, *130*, 5428-5429.

Duong, B., Seraphin, S., Wang, L., Peng, Y., & Xin, H. (2011) Production of predominantly semiconducting double-walled carbon nanotubes, *Carbon, 49*, 3512-3521.

Duong, B., Gangopadhyay, P., Seraphin, S., & Thomas, J. (2012) Multiwall carbon nanotubes grown by thermocatalytic carbonization of polyacrylonitrile, *Carbon*, in press.

Dresselhaus, M. S., Dresselhaus, G., & Eklund, P. C. (1996). *Science of Fullerenes and Carbon Nanotubes*, San Diego, USA: Academic.

Dresselhaus, M. S., Dresselhaus, G., & Saito, R., Jorio, A. (2005) Raman spectroscopy of carbon nanotubes, *Phys. Reports, 409*, 47-99.

Dresselhaus, M. S., Jorio, A., Hofmann, M., Dresselhaus, G., & Saito, R. (2010) Perspectives on carbon nanotubes and graphene Raman spectroscopy, *Nano Lett.*, *10*, 751-758.

Du, F., Qu, L., Xia, Z., Feng, L., & Dai, L. (2011) Membranes of Vertically-aligned Superlong Carbon Nanotubes, *Langmuir*, *27*, 8437-8443.

Ellis, M., (2012), Ph.D., Investigation of multiwalled carbon nanofiber-graphite layer composites and analysis of natural chalks, University of Arizona.

Ellis, M., Jutarosaga, T., Smith, S.M., Wei, Y., & Seraphin, S. (2012) Composite films of vertically aligned carbon nanofibers with graphite layer grown by low temperature, low pressure chemical vapor deposition, Manuscript in preparation.

Endo, M., Takeuchi, K., Igarashi, S., Kobori, K., Shiraishi, M., & Kroto, H.W. (1993). The production and structure of pyrolytic carbon nanotubes (PCNTs). *J. Phys. and Chem. of Solids*, *54*, 1841-1848.

Fan, S., Chapline, M., Frankline, N., Tombler, T., Cassel, A. M., & Dai, H. (1999) Self-oriented regular arrays of carbon nanotubes and their field emission devices, *Science*, *283*, 512

Franklin, N. R., & Dai, H. (2000) An enhanced CVD approach to extensive nanotube networks with directionality, *Adv. Mater.*, *12*, 890-894.

Gong, K., Chakrabarti, S., & Dai, L. (2008) Electrochemistry at carbon nanotube electrodes: Is the nanotube tip more active than the sidewall? *Angew. Chem., Int. Ed.*, *47*, 5446-5450.

Guo, T., Nikolaev, P., Thess, A., Colbert, D.T., & Smalley, R.E. (1995) Catalytic growth of single-walled nanotubes by laser vaporization. *Chem. Phys. Lett.*, *243*, 49-54.

Hata, K., Futaba, D.N., Mizuno, K., Namai, T., Yumura, M., & Iijima, S., (2004) Water-Assisted Highly Efficient Synthesis of Impurity-Free Single-Walled Carbon Nanotubes, *Science*, *306*, 1362-1364.

Hofmann, S., Csanyi, G., Ferrari, A.C., Payne, M.C., & Robertson, J. (2005) Surface Diffusion: The Low Activation Energy Path for Nanotube Growth. *Phys. Rev. Lett.*, *95*, 036101-036104.

Honda, S., Lee, K., Aoki, K., Hirao, T., Oura, K., & Katayama, M. (2006) Low-temperature synthesis of aligned carbon nanofibers on glass substrates by inductively coupled plasma chemical vapor deposition. *Japanese J. Appl. Phys.*, *45*, 5326-5328.

Huang, J., Liu, Y., & You, T. (2010) Carbon nanofiber based electrochemical biosensors: a review. *Anal. Methods*, *2*, 202-211.

Huang, S. M., Cai, Q., Chen, J., Qian Y., & Zhang, L. J. (2009) Metal - catalyst-free growth of single-walled carbon nanotubes on substrates. *J. Am. Chem. Soc.*, *131*, 2094-2095.

Hughes, T.V., & Chambers, C.R. (1889) Manufacture of carbon filaments, 480.

Iijima, S. (1991) Helical microtubles of graphitic carbon. *Nature 354*, 56-58.

Jang, J.W., Lee, C.E., Oh, C.I., & Lee, C.J. (2005) Hydrogen storage capacity of different carbon nanostructures in ambient conditions. *J Appl. Phys. 98*, 074316-3.

Jeong, G. H., Yamazaki, A., Suzuki, S., Yoshimura, H., Kobayashi, Y., & Homma, Y. (2005) Cobalt-filled apoferritin for suspended single-walled carbon nanotube growth with narrow diameter distribution *J. Am. Chem. Soc*., *127*, 8238-8239.

Jiao, J., & Seraphin, S. (1998) Tailoring carbon nanoclusters to desired morphologies. *J. Mater. Res.*, *13*, 2438-2444.

Jishi, R. A., Venkataraman, L., Dresselhaus, M. S., & Dresselhaus, G. (1993) Phonon modes in carbon nanotubes, *Chem. Phys. Lett., 209*, 77-82.

Jorio, A., Saito, R., Hafner, J. H., Lieber, C. M., Hunter, M., McClure, T., Dresselhaus, G., & Dresselhaus, M. S. (2001) Structural (n, m) determination of isolated single-wall carbon nanotubes by resonant Raman scattering, *Phys. Rev. Lett.*, 2001, *86*, 1118-1121.

José-Yacamán, M.; Miki-Yoshida, M.; Rendón, L., & Santiesteban, J. G. (1993). Catalytic growth of carbon microtubules with fullerene structure. *Appl. Phys. Lett*., *62*, 657-659.

Jousseaume, V., Cuzzocrea, J., Bernier, N., & Renard, V.T. (2011) Few graphene layers/carbon nanotube composites grown

at complementary-metal-oxide-semiconductor compatible temperature. *Appl. Phys. Lett. 98*, 123103-1,123103-3.

Jutarosaga, T., Seraphin, S., Smith, S. M., & Wei, Y. (2006) Effect of RF-PECVD synthesis conditions on the carbon nanotube growth, *Proc. Micro. Soc. America*

Kondo, D., Sato, S., & Awano, Y. (2008) Self-organization of novel carbon composite structure: graphene multi-layers combined perpendicularly with aligned carbon nanotubes. *Appl. Phys. Express 1*, 074003-1,074003-3.

Kong, J., Soh, H., Quate, C. F., & Dai, H. (1998) Synthesis of individual single-walled carbon nanotubes on patterned silicon wafers, *Nature*, *395*, 878-881.

Kroto, H.W., Heath, J.R., O'Brien, S.C., Curl, R.F., & Smalley, R.E. (1985) C 60: Buckminsterfullerene. *Nature 318*, 162-163.

Kumar, M., & Ando, Y. (2010) Chemical vapor deposition of carbon nanotubes: a review on growth mechanism and mass production, *J. Nanosci. Nanotechnol.*, *10*(6), 3739-3758.

Kurti, J., Kresse, G., & Kuzmany, H. (1998) First-principles calculations of the radial breathing mode of single-wall carbon nanotubes, *Phys. Rev. B*, *58*, R8869-R8872.

Labunov, V.A., Shulitski, B.G., Prudnikava, A.L., Shaman, Y.P., Basaev, A.S. (2010) Composite nanostructure of vertically aligned carbon nanotube array and planar graphite layer obtained by the injection CVD method. *Semiconductor Phys., Quantum Electronics and Optoelectronics*, 13, 137-141.

Lee, C.J., Son, K.H., Park, J., Yoo, J.E., Huh, Y., & Lee, J.Y. (2001) Low temperature growth of vertically aligned carbon nanotubes by thermal chemical vapor deposition. *Chem. Phys. Lett.*, *338*, 113-117.

Li, Q., Yan, H., Zhang, J., & Liu, Z. (2004) Effect of hydrocarbons precursors on the formation of carbon nanotubes in chemical vapor deposition, *Carbon*, *42*, 829-835.

Li, W. Z., Xie, S., Qian, L. X., Chang, B. H., Zou, B. S., Zhou, W. Y., Zhao, R. A., & Wang G. (1996) Large-scale synthesis of aligned carbon nanotubes, *Science*, 274, 1701.

Li, Y., Cui, R., Ding, L., Liu, Y., Zhou, W., Zhang, Y., Jin, Z., Peng, F., & Liu J. (2010) How catalysts affect the growth of single-walled carbon nanotubes on substrates, *Adv. Mater.*, *22*, 1508-1515.

Linares, A., Canalda, J.C., Cagiao, M.E., Garcia-Gutierrez, M.C., Nogales, A., Martin-Gullon, I., et al. (2008) Broad-band electrical conductivity of high density polyethylene nanocomposites with carbon nanoadditives: multiwall carbon nanotubes and carbon nanofibers. *Macromolecules*, *41*, 7090-7097.

Liu, Y., Pan, C., & Wang, J. (2004) Raman spectra of carbon nanotubes and nanofibers prepared by ethanol flames. *J. Mater. Sci.*, *39*, 1091-1094.

Liu, B., Ren. W., Gao, L. B., Li, S. S., Pei, S. F., Liu, C., Jiang, C. B., & Cheng, H. M. (2009) Metal-catalyst-free growth of single-walled carbon nanotubes. *J. Am. Chem. Soc.*, *131*, 2082-2083.

Lu, C.G., & Liu, J. (2006) Controlling the diameter of carbon nanotubes in chemical vapor deposition method by carbon feeding. *J. Phys. Chem. B*, *110*, 20254-20257.

Ma, X., Wang, E., Zhou, W., Jefferson, D.A., Chen, J., Deng, S., et al. (1999) Polymerized carbon nanobells and their field-emission properties. *Appl. Phys. Lett.*, *75*, 3105-3107.

Mahan, G.D. (2002) Oscillations of a thin hollow cylinder: carbon nanotubes, *Phys. Rev. B*, *65*, 235402.1-7.

Malesevic, A., Chen, H., Hauffman, T., Vanhulsel, A., Terryn, H., & Van Haesendonck, C. (2007) Study of the catalyst evolution during annealing preceding the growth of carbon nanotubes by microwave plasma-enhanced chemical vapor depostion. *Nanotechnology*, *18*, 455602-455610.

Melechko, A.V., Merkulov, V.I., McKnight, T.E., Guillorn, M.A., Klein, K.L., Lowndes, D.H., et al. (2005) Vertically aligned carbon nanofibers and related structures: controlled synthesis and directed assembly. *J. Appl. Phys., 97*, 041301-39.

Miyauchi, Y. H., Chiashi, S. H., Murakami, Y., Hayashida, Y., & Maruyama, S. (2004)

Fluorescence spectroscopy of single-walled carbon nanotubes synthesized from alcohol, *Chem. Phys. Lett.*, 2004, *387*, 198-203.

Nessim, G.D. (2010) Properties, synthesis, and growth mechanisms of carbon nanotubes with special focus on thermal chemical vapor deposition. *Nanoscale, 2*, 1306-1323.

Nikolaev, P., Bronikowski, M. J., Bradley, R. K., Rohmund, F., Colbert, D. T., Smith, K. A., & Smalley, R. E. (1999) Gas-phase catalytic growth of single-walled carbon nanotubes from carbon monoxide, *Chem. Phys. Lett.*, *313*, 91-97.

Novoselov, K.S., Geim, A.K., Morozov, S.V., Jiang, D., Zhang, Y., Dubonos, S.V., et al. (2004) Electric field effect in atomically thin carbon films. *Science, 306*, 666-669.

Park, K.H., Yim, J.H., Lee, S., & Koh, K.H. (2005) High current field emission from carbon nanofiber films grown using electroplated Ni catalyst. *J. Vacuum Sci. & Tech. B: Microelectronics and Nanometer Structures, 23*, 776-780.

Poa, C.H., Henley, S.J., Chen, G.Y., Adikaari, A.A., Giusca, C.E., & Silva, S.R. (2005) Growth and field emission properties of vertically aligned carbon nanofibers. *J. Appl. Phys., 97*, 114308-1,114308-6.

Rao, M., Richter, E., Bandow, S., Chase, B., Eklund, P. C., Williams, K. A., Fang, S., Subbaswamy, K. R., Menon, M., Thess, A., Smalley, R. E., Dresselhaus, G., & Dresselhaus, M. S. (1997) Diameter-selective Raman scattering from vibrational modes in carbon nanotubes, *Science*, *275*, 187-191.

Reynolds, C., Doung, B., & Seraphin, S. (2010) Effects of hydrogen flow rate on carbon nanotube growth, *J. Undergraduate Research in Physics, http://www.jurp.org/2010/ms115_082710.pdf*

Sanchez-Portal, D., Artacho, E., Soler, J. M., Rubio, A., & Ordejon, P. (1999) Ab initio structural, elastic, and vibrational properties of carbon nanotubes, *Phys. Rev. B, 59*, 12678-12688.

Satiskumar, B. C., Govindaraj, A., & Rao, C.N.R. (1999). Bundles of aligned carbon nanotubes obtained by the pyrolysis of ferrocene–hydrocarbon mixtures: role of the metal nanoparticles produced in situ. *Chem. Phys. Lett., 307*, 158-162.

Sen, R., Govindaraj, A., & Rao, C. N. R. (1997) Carbon nanotubes by the metallocene route, *Chem. Phys. Lett., 267*, 276-280.

Sivakumar, V.M., Abdul Rahman Mohamed, Ahmad Zuhairi Abdullah, & Siang-Piao, Chai. (2010) Role of reaction and factors of carbon nanotubes growth in chemical vapour decomposition process using methane—a highlight. *J. Nanomater.*, doi:10.1155/2010/395191

Sun, X., Li, K., Wu, R., Wilhite, P., Saito, T., Gao, J., et al. (2010) The effect of catalysts and underlayer metals on the properties of PECVD-grown carbon nanostructures. *Nanotechnology*, *21*, 045201-045206.

Sung, W.Y., Kim, W.J., Lee, H.Y., & Kim, Y.H. (2008) Field emission characteristics of carbon nanofibers grown on copper micro-tips at low temperature. *Vacuum*, *82*, 551-555.

Sveningsson, M., Morjan, R.E., Nerushev, O., & Campbell, E.E.B. (2004) Electron field emission from multi-walled carbon nanotubes. *Carbon*, *42*, 1165-1168.

Takagi, D., Kobayashi, Y., Hibirio, H., Suzuki, S., & Homma, Y. (2008) Mechanism of gold-catalyzed carbon material growth. *Nano Lett*., *8*, 832-835.

Takeda, G., Pan, L., Akita, S., & Nakayama, Y. (2005) Vertically aligned carbon nanotubes grown at low temperatures for use in displays. *Japanese J. Appl. Phys., 44*, 5642-5645.

Valentini, L., Cantalini, C., Armentano, I., Kenny, J.M., Lozzi, L., & Santucci, S. (2004) Highly sensitive and selective sensors based on carbon nanotubes thin films for molecular detection. *Diamond and Related Materials, 13*, 1301-1305.

Vera-Agullo, J., Glória-Pereira, A., Varela-Rizo, H., Gonzalez, J.L., & Martin-Gullon, I. (2009) Comparative study of the dispersion and functional properties of multiwall carbon nanotubes and helical-ribbon carbon nanofibers in polyester nanocomposites. *Composites Sci. Technol., 69*, 1521-1532.

Wang, Q.H., Setlur, A.A., Lauerhaas, J.M., Dai, J.Y., Seelig, E.W., & Chang, R.P.H. (1998) A nanotube-based field-emission

flat panel display. *Appl. Phys. Lett.*, *72*, 2912-2913.

Wang, Y., Alsmeyer, D., & McCreery, R. (1990) Raman spectroscopy of carbon materials: structural basis of observed spectra, *Chem. Mater.*, *2*, 557-563.

Wei, B.Q., Vajtai, R., Jung, Y., Ward, J., Zhang, R., Ramanath, G., & Ajayan, P.M. (2002) Organized assembly of carbon nanotubes, *Nature*, *416*, 495-496.

Wu, L., Zhang, X., & Ju, H. (2007) Detection of NADH and ethanol based on catalytic activity of soluble carbon nanofiber with low overpotential. *Anal. Chem.*, *79*, 453-458.

Yen, J.H., Leu, I.C., Lin, C.C., & Hon, M.H. (2004) Effect of catalyst pretreatment on the growth of carbon nanotubes. *Diamond and Related Materials*, *13*, 1237-1241.

Yuan, D. N., Ding, L., Chu, H. B., Feng, Y. Y., McNicholas, T. P., & Liu, J. (2008) Horizontally aligned single-walled carbon nanotube on quartz from a large variety of metal catalysts, *Nano Lett.*, *8*, 2576-2579.

Zhang, D., Kandadai, M.A., Cech. J., Roth. S., & Curran, S.A. (2006) Poly(L-lactide) (PLLA)/multiwalled carbon nanotube (MWCNT) composite : characterization and ciocompatibility cvaluation. *J. Phys.Chem. B*, *110*, 12910-12915.

Zhou, W. W., Han, Z. Y., Wang, J. Y., Zhang, Y., Jin, Z., Sun, X., Zhang, Y. W., Yan, C. H., & Li, Y. (2006) Copper catalyzing growth of single-walled carbon nanotubes on substrates. *Nano Lett.*, *6*, 2987-2990.

Zhou, W., Ding, L., & Liu, J. (2009) Role of Catalysts in the Surface Synthesis of Single-Walled Carbon Nanotubes *Nano Res.*, *2*, 593-598.